

Evolution of air-sea CO₂ flux during ARAMIS, EGEE and ROAM

ABSTRACT-

The aim of this study is to compare evolution of the CO₂ in two different areas of the tropical Atlantic Ocean. We investigate the spatial and temporal variability of CO₂ fluxes, Total Alkalinity (TA), Dissolved Inorganic Carbon (DIC) and hydrological parameters (Salinity and Temperature) in the western and eastern tropical Atlantic for three years (2005-2006-2007), using the data collected during the ARAMIS 7, 8 and 10, EGEE and ROAM cruises (2019-2020). Our results showed that Sea Surface Salinity (SSS), Sea Surface Temperature (SST), TA and DIC are higher on average in the western area than in the eastern tropical Atlantic, except the oceanic CO₂ fugacity (fCO_{2sw}). A north-south gradient is observed with high values in the south of the Equator and low values in the north. This gradient is due to the Equatorial upwelling, which upwelled CO₂-rich deep water to the surface; in addition, the Guinea current (GC) transports low salinity and parameters of carbon in the eastern area and Amazon outflow at West decreases the concentration of these parameters. On average, the western area was a sink of 0.34 mmol.m⁻².d⁻¹ and the eastern basin a source of 1.15 mmol.m⁻².d⁻¹. During ROAM cruises, air-sea CO₂ flux was ten times higher than during all the EGEE cruises and more for all ARAMIS cruises.

Keywords--- CO₂ Fluxes, Fugacity, Total Alkalinity, Dissolved Inorganic Carbon.

1. INTRODUCTION

Ocean plays a great role in the global climate regulation. In 2008, CO₂ emission from fuel combustion, cement production and gas flaring were about 8.7±0.5 Pg.C.yr⁻¹ (pentagram of carbon per year) [1]. In addition, some climatic models estimate of carbon uptake rate of biosphere and ocean were respectively 4.7±1.2 and 2.3±0.4 Pg.C.yr⁻¹. Then, Ocean has absorbed around the quarter of anthropogenic CO₂[2–5]. Many cruises conducted in the Atlantic Ocean highlighted its tropical belt acts globally as a CO₂ source for the atmosphere. Takahashi [6] showed that this area is a source of about 0.10 PgC.yr⁻¹ (0.26mmol.m⁻².d⁻¹).

The behavior of the tropical Atlantic is not homogeneous. Several areas act as a CO₂ sinks. Indeed, some authors [7] highlighted the western tropical Atlantic Ocean is a CO₂ sink for the atmosphere. It becomes therefore important to understand the changes occurring in the tropical Atlantic. This could be done through a good quantification of the air-sea CO₂ fluxes. Using the opportunities offered by the trips of the merchant vessel the Monte Olivia between France and Brazil, hydrological and carbon parameters measurements have been done between 2002 and 2008 during the ARAMIS project. The purpose of this project was to provide a long-term

survey for thermohaline structures in the tropical Atlantic Ocean [8]. In the eastern tropical Atlantic, between 2005 and 2007 the EGEE cruises were conducted in the Gulf of Guinea in order to study the ocean surface layer, the interactions ocean-atmosphere and also the ocean dynamic [9]. Also, during the ROAM cruises from 2018 to 2020 seawater samples were collected in order to study the impact of the carbonate system on the phytoplankton in Ivorian coastal area.

The aim of this work is to compare the CO₂ fluxes and the distribution of the carbon parameters during ARAMIS, EGEE and ROAM cruises. Moreover, these distributions could improve our knowledge of the factors impacting these parameters concentrations.

2. DATA AND METHODS

2.1 Data

The data were collected in the Gulf of Guinea during both cruises such as EGEE and ROAM cruises, and also the ARAMIS project. The others data used were provided by the climatology of [6].

The ARAMIS routes were between 35°N, 15°W (North-West of the African Coast) and 20°S, 40°W (near the South American East Coast) in spring and autumn (figure 1). It was a set of 12 cruises started in 2002 to end in 2008 with two cruises per year. In this paper only the ARAMIS 7, 8 and 10 data are used. For more information about ARAMIS data you can consult[8]. During the EGEE program, six cruises took place between 2005 and 2007 with two per year in the eastern tropical Atlantic[10](Table 1). An example of the track during the EGEE cruises is presented on figure 1. During these cruises, seawater samples were collected at different hydrological stations and analyzed for TA and DIC. Temperature and salinity were also measured on the same seawater as the samples for DIC and TA. The accuracy of DIC and TA in this work reaches $\pm 2 \mu\text{mol}\cdot\text{kg}^{-1}$.

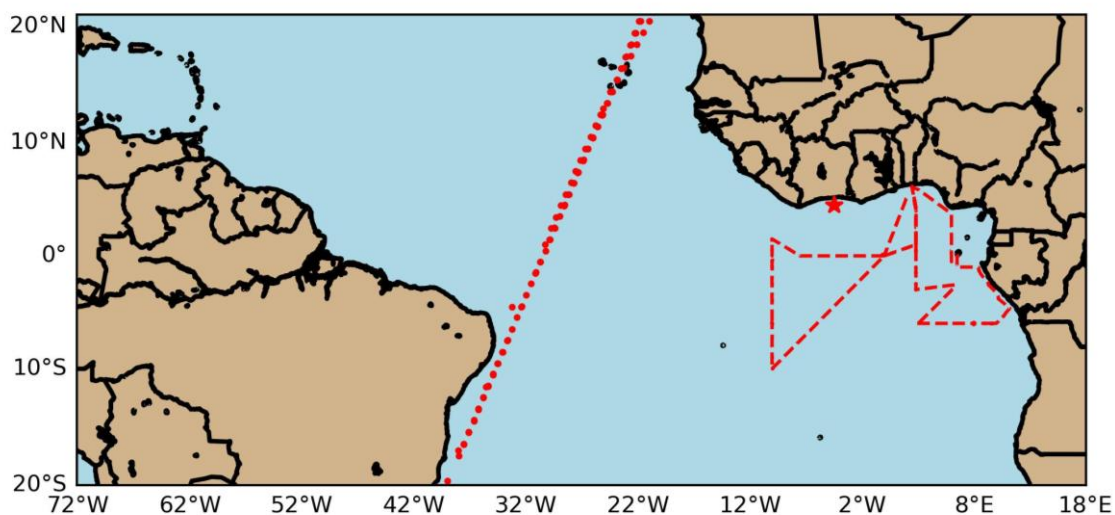


Figure 1: Mean tracks of Monte Olivia (ARAMIS ROUTE in red dot) and EGEE (EGEE 1 ROUTE in red dash line) voyages during which oceanographic samples were done. The red star indicates the ROAM samples station.

Table 1: List of the different cruises during which carbon and hydrological measurements have been made.

Cruises	Dates	Measurements	Zone
EGEE 1	7 June-6 July 2005	TA, DIC, SSS, SST	Gulf of Guinea
EGEE 2	29 August-30 September 2005	TA, DIC, SSS, SST	Gulf of Guinea
EGEE 3	27 May-7 July 2006	TA, DIC, SSS, SST	Gulf of Guinea
EGEE 4	19 November-1 December 2006	TA, DIC, SSS, SST	Gulf of Guinea
EGEE 5	6 June-3 July 2007	TA, DIC, SSS, SST	Gulf of Guinea
EGEE 6	1 ^{er} -30 September 2007	TA, DIC, SSS, SST	Gulf of Guinea
Aramis 7	5-13 October 2005	TA, DIC, SSS, SST	France-Brazil
Aramis 8	8-14 Mai 2006	TA, DIC, SSS, SST	France- Brazil
Aramis 10	23-29 April 2007	TA, DIC, SSS, SST	France- Brazil
ROAM	23 rd October 2018- 05 th December 2020	TA, DIC, SSS, SST	Gulf of Guinea

TA: Total Alkalinity; DIC: Dissolved Inorganic Carbon; SSS: Sea Surface Salinity; SST: Sea Surface Temperature

2.2. Methods

The hydrological data were made using a SEABIRD ThermoSalinoGraph(TSG) embarked on board the ship. A surface water sample is taken in front of the vessel during the cruises. Surface temperature and salinity were recorded automatically underway. These measurements were validated with the CTD (Conductivity, Temperature, Depth profiler) and XBT (eXpendableBathyThermograph) launching. More information about ARAMIS cruises XBT and CTD were available in [8]. TA and DIC method acquisition consisted in sampling seawater with Niskin bottles or pumping it at the ship front. The sampling is realized in order to reduce pollution rate. The samples were then analyzed in laboratory in order to determine TA and DIC. The analysis was based on potentiometric method [11]. The two equivalent points obtained were calculated using the code published by Dickson and Goyet [12]. The Certified Reference Materials (CRM) provided by Prof. A. Dickson of Scripps Institutions of Oceanography of San Diego in USA, was used for calibration. The accuracy of DIC and TA estimated at $\pm 2 \mu\text{mol.kg}^{-1}$ was the one recommended internationally (WOCE/JGOFS programs).

A Multilinear regression was established between DIC, SSS and SST with coefficient of correlation (R^2). Multiple linear regression is a statistical technique used to analyze the relationship between two or more independent variables and a dependent variable.

2.3. Oceanic $f\text{CO}_2$ ($f\text{CO}_{2\text{sw}}$) and CO_2 Flux Measurement

The $f\text{CO}_{2\text{sw}}$ used in this paper have been computed with the code developed by Lewis and Wallace [13]. This code is based on the set of some main parameters (SSS, SST, TA and DIC) and optional ones (pressure, phosphate, silicon and pH...). These parameters are the code input data. Then the choice of other parameters (dissociation constants K_1 and K_2 , solubility constant K_0 , KHSO_4 values and sulphites and fluorite concentration) is made to obtain the output data like the oceanic $f\text{CO}_2$.

The air-sea CO_2 fluxes (F) is calculated using the following expression: $F = K \Delta f\text{CO}_2$ where K is the gas exchange coefficient and $\Delta f\text{CO}_2$ the difference between seawater $f\text{CO}_2$ and atmospheric $f\text{CO}_2$. The atmospheric $f\text{CO}_2$ are derived from the estimate of Prather et al. [14]. The values were respectively for the years 2005, 2006, 2007 and 2020 respectively 378.7, 380.8, 382.7 and 417 μatm .

3. RESULTS and DISCUSSIONS

3.1 - Hydrological Parameters Distribution

The hydrological parameters observed during ARAMIS are on average higher than those measured in the eastern area (Table 2). And a north-south gradient is observed in these parameters' distribution. During EGEE cruises, the south Equator (0-10°S) exhibits high values of SSS (>35.5 psu) where as low values (<35.5 psu) are observed in the north. An opposite pattern is observed for the SST distribution with low values (<26 °C) in the south and high values in the north (>26°C). The same characteristics of the distribution are recorded during the autumn 2005 cruises in the western area (ARAMIS 7) for the hydrological parameters. In the spring (ARAMIS 8 and 10), the SSS distribution is identical to those of the others cruises however the SST is quite different. Indeed, SST is higher in the south Equator than in the north. Many factors could explain this difference. In the Gulf of Guinea, the strong desalinization in the north of the Equator is due to the rivers outflow and the high precipitation recorded during the data sampling [10]. The south area which is not under these phenomenon effects, exhibits an average SST lower of 1.5 °C relatively to the north and an average SSS higher of 0.75 psu. The sampling period during EGEE cruises was made during the upwelling season. During this phenomenon, cold and saltier deep-water rich in dissolve CO₂ is brought up to the surface. This explains the lower SST and higher SSS south Equator in the Gulf of Guinea. In the Western region, the higher SST and SSS are registered south Equator. The values are higher of 1 psu and 2°C respectively for SSS and SST with reference to the Eastern region (Table 2). The mean SST registered are higher than 26 °C. These high SST are explained by the warming of surface water when flowing westward through the South Equatorial Current (SEC) [15]. The average SSS calculated in the north of this basin is lower of 1 psu relatively to south. The higher discharge of Amazon River is registered during the springs (Figure 2)[16]. No North Brazilian Current (NBC) reversal is observed through the North Equatorial Counter Current (NECC) throughout this period. It rather flows northward towards Caribbean[17]. As regards, the NECC retroflects about 18°W through the Guinea Current (GC), hence the impossibility for this current to carry Amazonian fresh waters eastward. During ARAMIS cruises, the lowest SSS area is located around 5°N and associated with SST neighboring 28°C (Figure 2). Higher SST and lower SSS suggest the presence of ITCZ around 5°N during ARAMIS cruises. The mean position of this zone is located between 5°S and 5°N during the spring in the western basin. ITCZ could then be the explanation of the lower SSS north the western basin during the 2006 and 2007 spring. This zone is associated with high precipitations, which by dilution effect lower salinity. Further north in this same period, the lower SST could be due to the cooling of the north hemisphere winter. In autumn (October 2005), ITCZ was situated beyond 5°N. NBC during this period retroflects through the NECC so Amazon River discharge were low. Amazon waters all the same are carried eastward. ITCZ and Amazon discharge are the explanation of the lower SSS values registered between 2°N and 0°N during October 2005. The high temperatures recorded (>26°C) in 2006 in both areas were a characteristic of this year that has been hot in spring and summer. Despite on average SST seems very close during all the three cruises but highest temperatures (>28°C) were recorded from November 2018 to March 2019 in dry season along the coast. In the whole, the ROAM cruises

look warmest than others two cruises (Figure 3). Indeed, during this cruise the observed SSTs were relatively high compared to the two others cruises without the upwelling periods. As seen on the figure 3, the upwelling period was quite cold during ROAM.

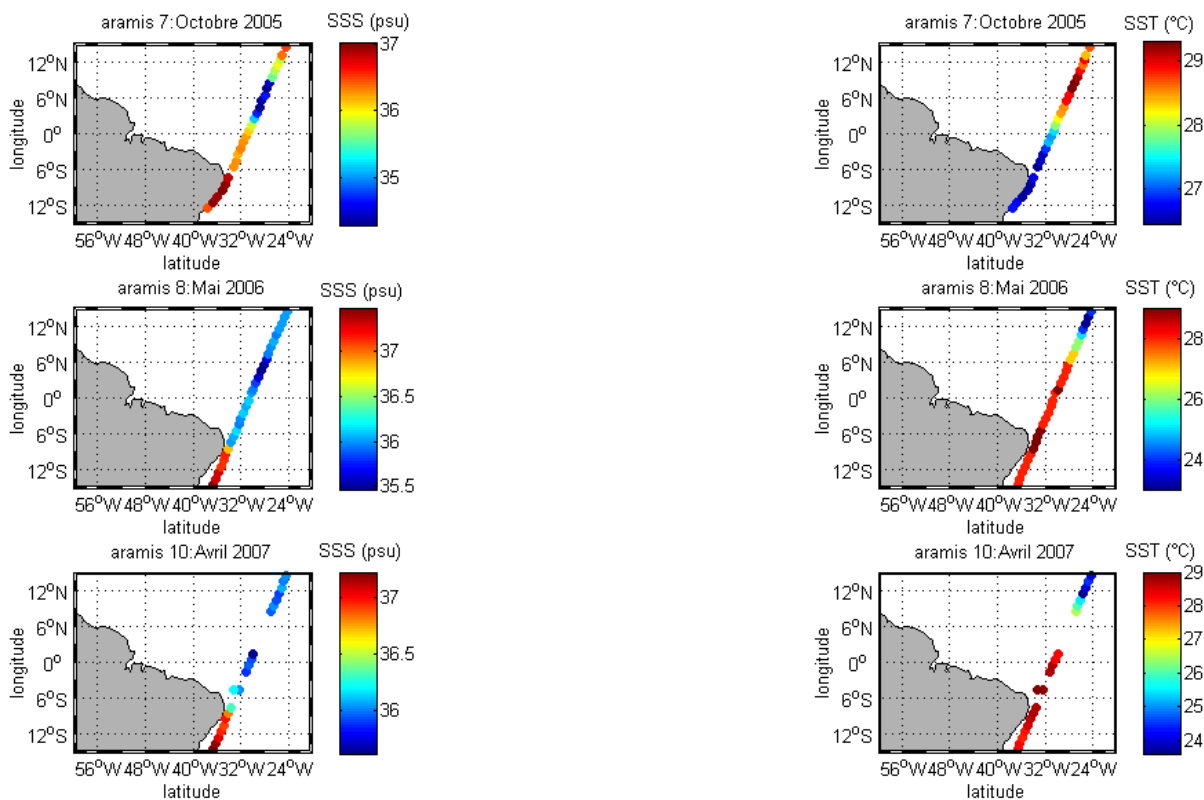


Figure 2: Distribution of Sea Surface Salinity (SSS) and Sea Surface Temperature (SST) during ARAMIS 7, 8 and 10 cruises.

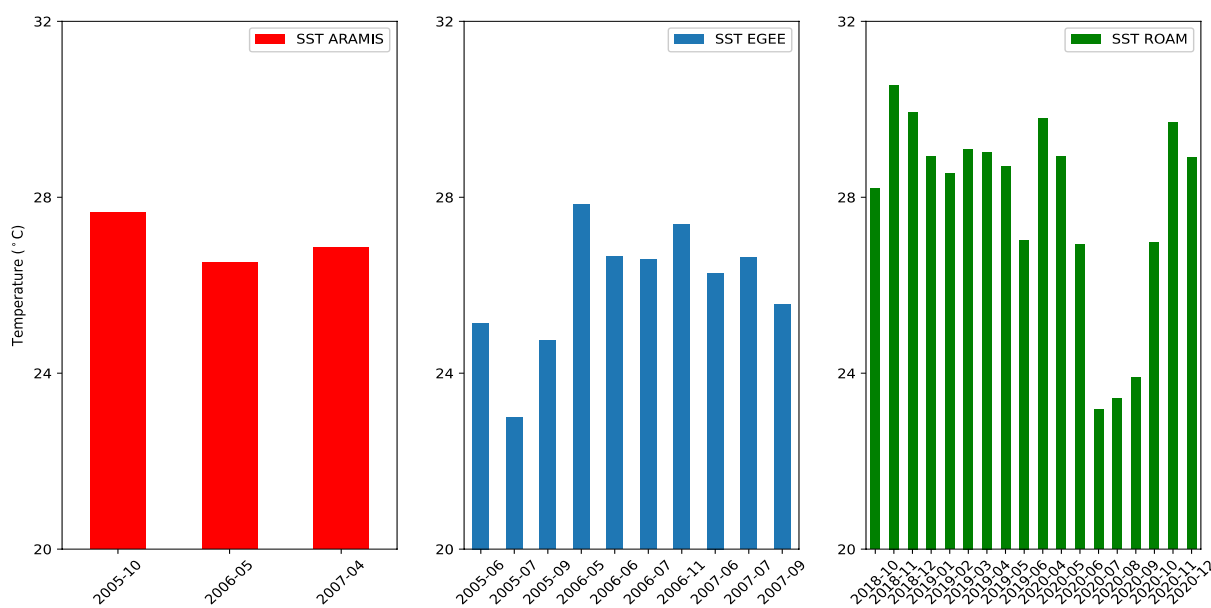


Figure 3: monthly mean SST during ARAMIS, EGEE and ROAM cruises

Table 2: Mean values of SSS, SST, TA, DIC and fCO_{2sw} during EGEE, ROAM and ARAMIS cruises. The values were computed for the north and south part of Tropical Atlantic Ocean Eastern and Western areas.

		SSS (psu)	SST (°C)	TA ($\mu\text{mol.kg}^{-1}$)	DIC ($\mu\text{mol.kg}^{-1}$)	fCO_{2sw} (μatm)
EGEE	south	35.58	25.32	2334.86	2027.24	406.66
	north	34.87	26.79	2285.40	1961.92	375.46
ARAMIS	south	36.59	27.88	2401.87	2042.04	386.81
	north	35.63	27.49	2333.62	1985.48	367.07
ROAM	north	33.20	27.63	2213.13	2005.91	656.33

3.2 – Distribution of Carbon Parameters (TA and DIC)

According to Millero et al. [18], the latitudinal distribution of TA in the surface waters always follows those of salinity. This is due to the fact that, TA which is an essential component of ocean is highly correlated to salinity. Some authors like [19], [20] and [21] have found robust relationships between TA and SSS. For instance, during the EGEE cruises, 96% of TA variations depended on the SSS [10]. It appeared a gradient in SSS and TA distribution. In addition, in the western region, SSS and TA, on average, are higher than SSS and TA in the eastern area. The mean difference between western and eastern TA is $55.39 \mu\text{mol.kg}^{-1}$. However, for the ROAM data TA-SSS, no relationships were found using two parameters because the samples were collected very close to coast because the coastal ocean dynamics are not like the open ocean.

The DIC variability depends on the salinity and also surface temperature variation [22]. Other phenomenon like biological and thermodynamic factors also impact DIC variability. The DIC values measured during EGEE cruises are on average lower than those observed during ARAMIS cruises. On average, the difference of DIC between the two areas is more important in the north ($26.24 \mu\text{mol.kg}^{-1}$) than in the south ($8.64 \mu\text{mol.kg}^{-1}$). Considering the double regression relationship determined by Koffi et al. [10] with EGEE data:

$$DIC = (51.71 \pm 2.16) * SSS + (-12.79 \pm 0.89) * SST + (507.82 \pm 91.32); R^2 = 0.90,$$

it is noticed that DIC variation is explained at 90% by salinity and temperature effects. The standard error on DIC is $\pm 16.6 \mu\text{mol.kg}^{-1}$. During EGEE cruises, SST was relatively low in the south Equator (25.15°C on average) compared to the north (26.64°C on average). The SST coefficient is negative suggests that low temperatures and high salinities; this is associated with high carbon concentration (high DIC). This corresponds to the upwelling regime observed in the south of the Equator. In the north, the low SSS and high SST recorded induce a drop in DIC, hence the low values observed. With ARAMIS data, the following relationship was determined:

$$DIC = (52.49 \pm 1.78) * SSS - (6.57 \pm 0.79) * SST + (302.47 \pm 70.17); R^2 = 0.93.$$

DIC variability during the three cruises is explained at 93% by temperature and salinity. The hydrological parameters distribution in the western region enables dividing it into three areas along the ship's tracks: A, B, C. The zone A ranges from 15°S to 3°N . In this region, on average relatively SSS (>35.8 psu) and SST ($>28^\circ\text{C}$) are higher in spring and autumn. For the second area B, SSS are lower (<35.8 psu) and SST higher ($>27^\circ\text{C}$ on average) in spring and autumn. This area ranges from 3°N to 7°N and covers the NECC. Beyond 7°N , it is the C area which covers the NEC. High SSS (>35.9 psu on average) and SST ($>28^\circ\text{C}$ on average) are registered there in autumn. In spring the two hydrological parameters are lower (SSS <35.8 psu and SST $<28^\circ\text{C}$ on

average). The estimated error on the western relationship salinity slope is $\pm 1.78 \mu\text{mol.kg}^{-1}$. When applying it to the western relationship, the slope obtained is close to the relationship found in the eastern area.

However, as observed for TA-SSS using data from ROAM cruise, no relationships were found between DIC, SSS and SST because of the coastal ocean features that impact DIC spatial and temporal variability as presented by Vance [23]

3.3 - Distribution of Sea CO₂ Fugacity (fCO_{2sw})

The sea CO₂ fugacity (fCO_{2sw}) distribution is different of those of TA, DIC, SSS and SST. It is higher on average in the Gulf of Guinea than in the western area. The difference is more important in the south of the Equator where high values are observed in the Gulf of Guinea (406.66 μatm on average) (table 2). These values are associated with high SSS and low SST. These high values are due to the cold upwelled waters rich in CO₂. In the north of the Equator, according to [24], the high precipitations due to the position of ITCZ on the tropical Atlantic Ocean could affect the concentration of the CO₂ parameters in the north-west. The GC then transports these low concentrations eastwards in the ocean.

In the western region, the estimated mean value is around 376.94 μatm . The fCO_{2sw} values observed on the ships track vary according to the currents crossed. Between 15°S and 6°S in the BC, the mean value is 379.17 μatm . The fugacity then increases to reach 396.46 μatm between 6°S and 2°N in the SEC, and decreases beyond 2°N (362.37 μatm on average) in the NECC and NEC. During the spring, Amazon discharge is higher, the NECC retroflects near 18°W into the GC [17] and the ITCZ is located around 2°S [25]. Amazon waters cannot be encountered further east. The CO₂ undersaturation in this area up to 2°N could be explained by the cooling of the boreal winter. In the SEC, the high fCO_{2sw} encountered are due to the heating of the water both in spring and autumn (high SST). During the boreal spring, it is the autumn in the south hemisphere. The low fCO_{2sw} in the BC area are associated with high SST and SSS. Neither the heating nor the austral winter cooling could explain the CO₂ undersaturation. The Ship track in this area is close to the coast. The areas near the coasts are generally affected by biological activity. So, the low fCO_{2sw} in this region could be due to the consumption of CO₂. During the boreal autumn 2005 (austral spring), the fCO_{2sw} was low associated with high SST (>26°C) and higher SSS (>36 psu). The CO₂ undersaturation was due to the cooling of the austral winter. Between 2°N and 8°N, the hypothesis is that fCO_{2sw} variation is led by those of salinity. According to [16], during the France-Guyana cruises, fCO_{2sw} variability would have been highly correlated to salinity. In 2005 autumn, between 2°N and 8°N, salinity values were lower than 34.5 psu on average and this was due to ITCZ which was located there at this period of year [25]. The lower salinity areas are generally associated with lower TA, DIC and fCO_{2sw}. According to [17], NECC reaches its maximum velocities during the northern autumn in August. During this period, ITCZ is located at its northern position. Amazon River waters sometimes reaches 25°W-30°W, depending on NECC strength. The lower SSS and fCO_{2sw} during this period are the result of the ITCZ and the eastward propagation of Amazon River waters. The lower values of fCO_{2sw} associated with lower salinities in tropical Atlantic are due to ITCZ [26]. This zone reaches its southernmost position between March and April, and then migrates northward between July and August. This is consistent with the lower salinity values observed north 2°N in autumn (Figure 2). In the north of 10°N (NEC region), the higher fCO_{2sw} encountered are due to the higher temperature registered there. Low fCO_{2sw} (<390

μatm) are also registered in the southwest of the eastern basin and associated with higher SSS and SST. These values are consistent with the data collected in June 2006 at the buoy located at 10°W , 6°S [27]. This region of the Atlantic is isolated from precipitations and rivers outflow, that why the SSS is still high.

3.4 - Comparison of calculated and measured $f\text{CO}_{2\text{sw}}$ during ARAMIS cruises

Distribution of calculated and measured $f\text{CO}_{2\text{sw}}$ for different months is shown on a figure 4. In general, when moving away from the equator, the discrepancy between measured and calculated values becomes significant (Figure 4). An agreement is generally observed between measured and calculated values from 5°S to 5°N . Apart August and December 2008, the differences observed generally do not exceed $10 \mu\text{atm}$. In this area, SSS and SST vary inversely. The region beyond 5°S exhibits higher salinity ($>35.5 \text{ psu}$) and temperature lower than 27°C , which induces higher values of estimated DIC. DIC and $f\text{CO}_{2\text{sw}}$ depend on carbonate system variability and vary generally in the same ratio. Higher values of DIC then induce higher values of estimated $f\text{CO}_{2\text{sw}}$. That explains the higher discrepancy observed ($>20 \mu\text{atm}$) in this area. A different pattern is observed in April 2009. For this month, higher SSS are associated higher SST and a good agreement is observed between measured and estimated values from 15°S to 10°N . Between 5°N and 10°N , salinity increases and is lower than 35.5 psu for the other months. It is associated to higher values of SST ($>28^{\circ}\text{C}$). This induces lower estimated DIC. So, the measured DIC are lower than the estimated ones. Lefèvre et al. [16] showed that this is related to the lower salinities observed in the zone.

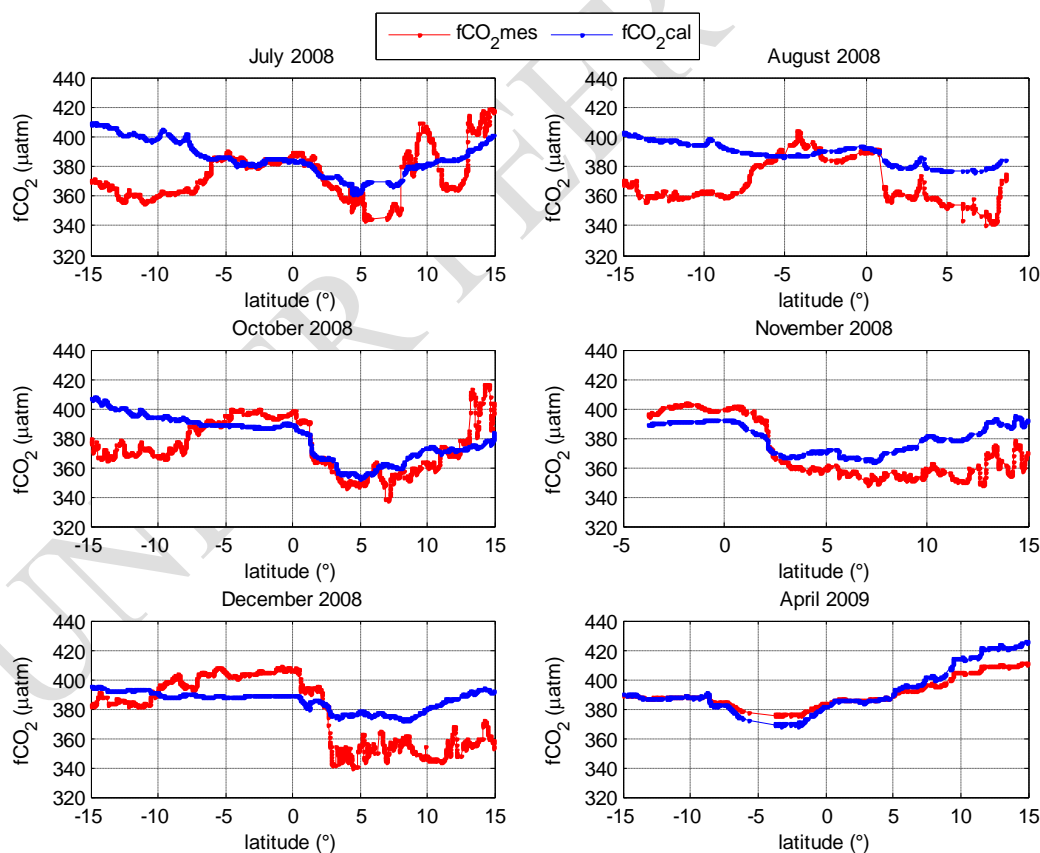


Figure 4. Calculated ($f\text{CO}_{2\text{cal}}$) and measured ($f\text{CO}_{2\text{mes}}$) sea CO_2 fugacity distribution along the monte Olivia track for different months. (July, August, October, November and December 2008; April 2009)

These authors showed that carbon parameters were strongly correlated to salinity in this region. These authors have determined TA-SSS and DIC-SSS relationships with data collected south 12°N and west 30°W during October 2007 Plumand and Amandes, August 2008 Transit cruises. Comparing measured and calculated $f\text{CO}_2$ values obtained from TA and DIC determined from these relationships, they showed that calculated values underestimate measured values for high $f\text{CO}_2$ associated to high salinity. This report is also observed when salinity is low. In November 2008, measured $f\text{CO}_{2\text{sw}}$ are higher than calculated ones for high salinity values (>35 psu). The seasonal and interannual variability of hydrological parameters could be another explanation of these discrepancies observed.

3.5 - Variability of air-sea CO_2 fluxes

According to Koffi et al.[24], in the eastern area of tropical Atlantic, the CO_2 gradient was due to the GC water transport and to the upwelling. For these authors, in the north of the Equator, GC transports eastward-unsalted waters due to precipitations contributing to the dilution and the decrease of CO_2 . Furthermore, in the south of the Equator, the air-sea CO_2 flux was mainly driven by the oceanic $f\text{CO}_2$ due to the CO_2 supply by upwelled waters. In the western area, ITCZ, Amazon outflow and winter cooling were responsible of the CO_2 undersaturation [7], [16].

Comparing the air-sea CO_2 fluxes in June 2005, 2006 and 2007, the release of CO_2 to the atmosphere is weak in 2006 in the eastern area. Indeed, in June 2006, SST was higher (-26.70°C) compared in June 2005 and 2007. This was due to the disconnection of the Equatorial cold tongue from the cold waters farther south in the eastern region [28]. The mean SSS was lower around 35.37 psu, which induces low values of DIC. This could be caused by the transport of water, which was in contact with the atmosphere long time enough to come close to equilibrium according to [5]. In the western region, the sink was twice important in May 2006 than in April 2007. For the same season (ARAMIS 8 and EGEE 3), the western region was a sink of $0.71 \text{ mmol.m}^{-2}.\text{d}^{-1}$ whereas the eastern region was a source of $1.55 \text{ mmol.m}^{-2}.\text{d}^{-1}$. The seasonal variability cannot be compared because of the lack of data.

Moreover, using data from ROAM cruises, air-sea CO_2 flux ($23.27 \text{ mmol.m}^{-2}.\text{d}^{-1}$) was ten times higher than during all the EGEE cruises ($2.3 \text{ mmol.m}^{-2}.\text{d}^{-1}$) and more for all ARAMIS ($-1 \text{ mmol.m}^{-2}.\text{d}^{-1}$). Indeed, the global average atmospheric $f\text{CO}_2$ rise more rapidly in the 2000s ($1.9 \mu\text{atm yr}^{-1}$) and 2010s ($2.4 \mu\text{atm yr}^{-1}$), while the global mean surface ocean $f\text{CO}_2$ increased $1.8 \mu\text{atm}$ per year in the 2000s and $2.1 \mu\text{atm}$ per year in the 2010s on average, suggesting a continuously increasing $\Delta f\text{CO}_2$ across the interface since 2000 [29]. Also, the entire western tropical Atlantic acts as a net annual CO_2 sink of $-1.6 \pm 1.0 \text{ mmol.m}^{-2}.\text{d}^{-1}$ despite a large spatial variability [30]. This result shows a net increase of the CO_2 sink in the western tropical Atlantic in comparison of the eastern area.

3.5 – The Flux Comparison with Takahashi Climatology

This sub-section highlights the differences between the CO_2 fluxes estimated during EGEE 3 in June 2006, ARAMIS 8 in May 2006 and the climatology of Takahashi et al. [6]. EGEE 3 and ARAMIS 8 are chosen because of the proximity of their data sampling. The EGEE 3 data, which were at proximate latitudes, but at different longitudes, have been averaged to take into account only this latitude. This climatology was referenced

to the year 2000 and has been built by averaging the CO₂ fluxes in our study areas previously defined. The climatology for the year 2006 presents both areas as CO₂ source for the atmosphere. The mean values respectively for the eastern and western region are respectively 1.23 and 1.63 mmol.m⁻².d⁻¹. The source observed with the climatology in the eastern area is in agreement with the one with the in-situ data. The climatology indicates that the western area was a source, which was not consistent with the in-situ data (Figure 5). In the south of the Equator (Figure 5B), the flux with the climatology in the western area (2.63 mmol.m⁻².d⁻¹) is higher than the one of the eastern area (1.58 mmol.m⁻².d⁻¹), which is different with the in-situ data. The in-situ data present the two areas as CO₂ sinks in the north of the Equator (Figure 5A) whereas for the climatology the north of the western area is a source of 0.38 mmol.m⁻².d⁻¹. This could be due to the coarse resolution (4° latitude x 5° longitude) used in the climatology, which tended to smooth the difference between northern and southern waters according to Koffi et al.[24]. Nevertheless, the flux gradient was slightly reproduced in the two areas by the climatology.

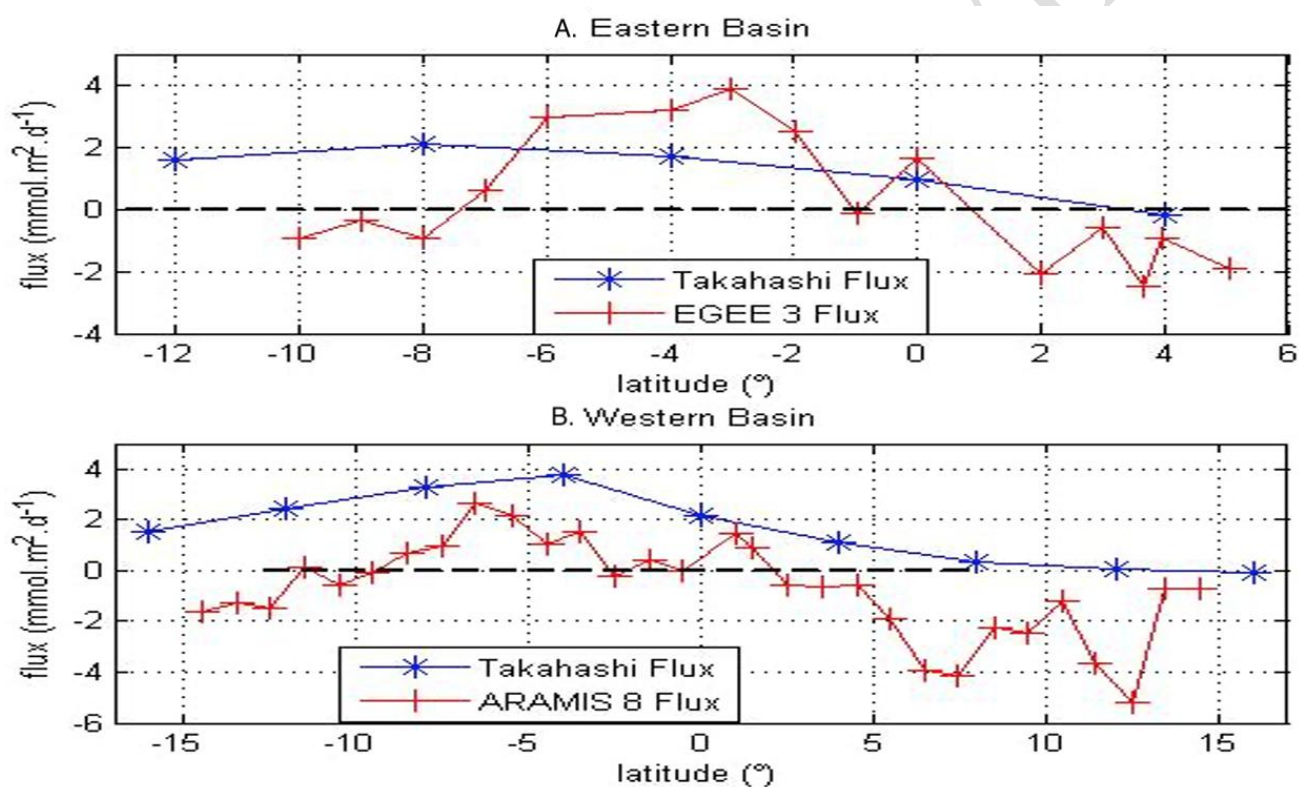


Figure 5: Latitudinal distributions of mean climatological (Takahashi) and calculated (EGEE 3 and ARAMIS 8) fluxes in the eastern basin (A) and the western basin (B).

4. CONCLUSION

This work was initiated to better assess the differences and the phenomenon responsible of the CO₂ flux and carbon variability in the western and eastern part of tropical Atlantic Ocean. Our results clearly show differences between the two regions. Except the air-sea CO₂ fugacity, all the parameters are higher in the western region than in the eastern on average. The distribution shows a north-south gradient. In the western basin,

SST and SSS are higher in the south of the Equator and lower north it during the spring. In autumn, this area displays the same structure to the eastern area with higher SST ($>26^{\circ}\text{C}$) [resp. Lower SSS (<35.5)] in the north of the Equator and lower SST [resp. higher SSS] south it. Our results show that TA is highly correlated to salinity. In the eastern region, the high values recorded in the south of the Equator are related to the cold upwelled waters rich in CO_2 and nutrients whereas in the north, waters transport by GC is responsible to the lower values. In the western region, in the north of the Equator, the lower values are due to ITCZ, winter cooling and Amazon outflow. The climatology of Takahashi underestimates the estimated values. The calculated values present the eastern area of tropical Atlantic as a source of $0.87\text{mmol}\cdot\text{m}^{-2}\cdot\text{d}^{-1}$ whereas the western region is a sink of $0.71\text{mmol}\cdot\text{m}^{-2}\cdot\text{d}^{-1}$ with EGEE 3 and ARAMIS 8 data, which was not consistent with the climatology. This climatology presents the western region as a source of $1.63\text{mmol}\cdot\text{m}^{-2}\cdot\text{d}^{-1}$. This could be due to the coarse resolution (4° latitude x 5° longitude) used in the climatology, which tended to smooth the difference between northern and southern waters according to the climatology. Nevertheless, the flux gradient was slightly reproduced in the two basins by the climatology. In addition, using data from ROAM cruises, air-sea CO_2 flux ($23.27\text{mmol}\cdot\text{m}^{-2}\cdot\text{d}^{-1}$) was ten times higher than during all the EGEE cruises ($2.3\text{mmol}\cdot\text{m}^{-2}\cdot\text{d}^{-1}$) and more for all ARAMIS ($-1\text{mmol}\cdot\text{m}^{-2}\cdot\text{d}^{-1}$). So, the coastal area exhibits more CO_2 release to the atmosphere than the open ocean. To understand the influence of the air-sea CO_2 flux along the coastal areas of the tropical Atlantic, it is important to observe, to monitor and to identify the impacts of ocean acidification on the marine ecosystems.

REFERENCES

1. Le Quéré C, Takahashi T, Buitenhuis ET, Rödenbeck C, Sutherland SC (2010) Impact of climate change and variability on the global oceanic sink of CO_2 . *Glob. Biogeochem. Cycles* 24:
2. Baker DF, Law RM, Gurney KR, Rayner P, Peylin P, Denning AS, Bousquet P, Bruhwiler L, Chen Y-H, Ciais P (2006) TransCom 3 inversion intercomparison: Impact of transport model errors on the interannual variability of regional CO_2 fluxes, 1988–2003. *Glob. Biogeochem. Cycles* 20:
3. Denman KL, Brasseur G, Chidthaisong A, et al (2007) Couplings between changes in the climate system and biogeochemistry. *Clim Change* 2007:541–584
4. Gruber N, Gloor M, Mikaloff Fletcher SE, Doney SC, Dutkiewicz S, Follows MJ, Gerber M, Jacobson AR, Joos F, Lindsay K (2009) Oceanic sources, sinks, and transport of atmospheric CO_2 . *Glob. Biogeochem. Cycles* 23:
5. Lefèvre N (2009) Low CO_2 concentrations in the Gulf of Guinea during the upwelling season in 2006. *Mar Chem* 113:93–101
6. Takahashi T, Sutherland SC, Wanninkhof R, Sweeney C, Feely RA, Chipman DW, Hales B, Friedrich G, Chavez F, Sabine C (2009) Climatological mean and decadal change in surface ocean pCO_2 , and net sea–air CO_2 flux over the global oceans. *Deep Sea Res Part II Top Stud Oceanogr* 56:554–577
7. Terner J-F, Oudot C, Dessier A, Diverres D (2000) A seasonal tropical sink for atmospheric CO_2 in the Atlantic Ocean: the role of the Amazon River discharge. *Mar Chem* 68:183–201
8. Tanguy Y, Arnault S, Lattes P (2010) Isothermal, mixed, and barrier layers in the subtropical and tropical Atlantic Ocean during the ARAMIS experiment. *Deep Sea Res Part Oceanogr Res Pap* 57:501–517
9. Redelsperger J-L, Thorncroft CD, Diedhiou A, Lebel T, Parker DJ, Polcher J (2006) African Monsoon Multidisciplinary Analysis: An international research project and field campaign. *Bull Am Meteorol Soc* 87:1739–1746
10. Koffi U, Lefèvre N, Kouadio G, Boutin J (2010) Surface CO_2 parameters and air–sea CO_2 flux distri-

- bution in the eastern equatorial Atlantic Ocean. *J Mar Syst* 82:135–144
11. Edmond JM (1970) High precision determination of titration alkalinity and total carbon dioxide content of sea water by potentiometric titration. In: *Deep Sea Res. Oceanogr. Abstr.* Elsevier, pp 737–750
 12. Dickson AG, Goyet C (1994) Handbook of methods for the analysis of the various parameters of the carbon dioxide system in sea water. Version 2. Oak Ridge National Lab., TN (United States)
 13. Lewis E, Wallace D (1998) Program developed for CO₂ system calculations. <https://doi.org/4735>
 14. Prather M, Flato G, Friedlingstein P, Jones C, Lamarque JF, Liao H, Rasch P (2013) Annex II: Climate system scenario tables. IPCC Clim. Change 2013 Phys. Sci. Basis
 15. Andrié C, Oudot C, Genthon C, Merlivat L (1986) CO₂ fluxes in the tropical Atlantic during FOCAL cruises. *J Geophys Res Oceans* 1978–2012 91:11741–11755
 16. Lefèvre N, Diverrès D, Gallois F (2010) Origin of CO₂ undersaturation in the western tropical Atlantic. *Tellus B* 62:595–607
 17. Stramma L, Schott F (1999) The mean flow field of the tropical Atlantic Ocean. *Deep Sea Res Part II Top Stud Oceanogr* 46:279–303
 18. Millero FJ, Lee K, Roche M (1998) Distribution of alkalinity in the surface waters of the major oceans. *Mar Chem* 60:111–130
 19. Lefèvre N, Guillot A, Beaumont L, Danguy T (2008) Variability of fCO₂ in the Eastern Tropical Atlantic from a moored buoy. *J. Geophys. Res. Oceans* 1978–2012 113:
 20. Friis K, Körtzinger A, Wallace DW (2003) The salinity normalization of marine inorganic carbon chemistry data. *Geophys. Res. Lett.* 30:
 21. Weiss R (1974) Carbon dioxide in water and seawater: the solubility of a non-ideal gas. *Mar Chem* 2:203–215
 22. Bakker DC, de Baar HJ, de Jong E (1999) The dependence on temperature and salinity of dissolved inorganic carbon in East Atlantic surface waters. *Mar Chem* 65:263–280
 23. Vance JM, Currie K, Zeldis J, Dillingham PW, Law CS (2022) An empirical MLR for estimating surface layer DIC and a comparative assessment to other gap-filling techniques for ocean carbon time series. *Biogeosciences* 19:241–269
 24. Koffi U, Kouadio G, Kouadio YK (2016) Estimates and Variability of the Air-Sea CO₂ Fluxes in the Gulf of Guinea during the 2005-2007 Period. *Open J Mar Sci* 06:11–22
 25. Gu G, Adler RF (2004) Seasonal evolution and variability associated with the West African monsoon system. *J Clim* 17:3364–3377
 26. Oudot C, Andrié C, Montel Y (1987) Evolution du CO₂ océanique et atmosphérique sur la période 1982–1984 dans l'Atlantique tropical. *Deep Sea Res Part Oceanogr Res Pap* 34:1107–1137
 27. Parard G, Lefèvre N, Boutin J (2010) Sea water fugacity of CO₂ at the PIRATA mooring at 6° S, 10° W. *Tellus B* 62:636–648
 28. Marin F, Caniaux G, Giordani H, Bourlès B, Gouriou Y, Key E (2009) Why were sea surface temperatures so different in the eastern equatorial Atlantic in June 2005 and 2006? *J Phys Oceanogr* 39:1416–1431
 29. Zhong G, Li X, Song J, Qu B, Wang F, Wang Y, Zhang B, Ma J, Yuan H, Duan L (2022) Global ocean CO₂ uptake dominated by the ENSO in the last thirty years.
 30. Monteiro T, Batista M, Henley S, Machado E da C, Araujo M, Kerr R (2022) Contrasting Sea-Air CO₂ Exchanges in the Western Tropical Atlantic Ocean. *Glob Biogeochem Cycles* 36:e2022GB007385